NUCLEAR DATA AND MEASUREMENTS SERIES

ANL/NDM-153

FAST NEUTRONS INCIDENT ON HAFNIUM

by

A. B. Smith

June, 2001

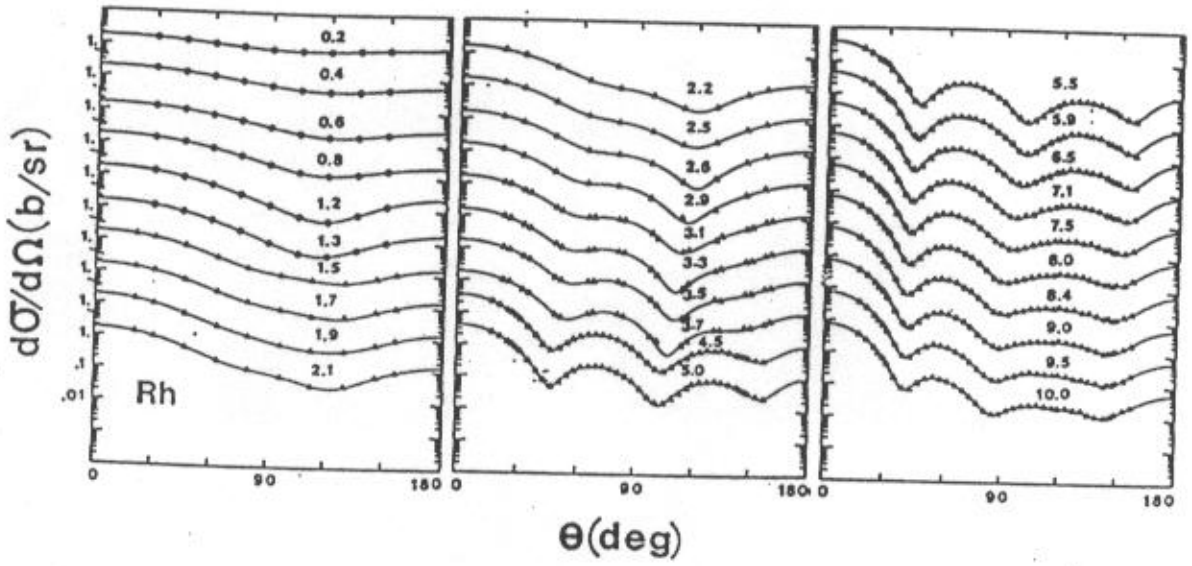

ARGONNE NATIONAL LABORATORY, ARGONNE, ILLINOIS

Operated by THE UNIVERSITY OF CHICAGO

for the U. S. DEPARTMENT OF ENERGY

under Contract W-31-109-Eng-38

Argonne National Laboratory, with facilities in the states of Illinois and Idaho, is owned by the United States Government, and operated by the University of Chicago under provisions of a contract with the Department of Energy.

Disclaimer

This report is available electronically at:
<http://www.doe.gov/bridge>.

It is also available for a processing fee to the U. S. Department of Energy and its contractors, in paper, from:

U. S. Department of Energy
Office of Scientific and Technical Information
P. O. Box 62
Oak Ridge, TN 37831-0062
Phone: (865) 576-8401
Fax: (865) 576-5728
E-mail: <reports@adonis.osti.gov>

Nuclear Data and Measurement Series

Reports in the Argonne National Laboratory Nuclear Data and Measurement Series present results of studies in the field of microscopic nuclear data. The primary objective of the series is the dissemination of information in the comprehensive form required for nuclear technology applications. This Series is devoted to: a) measured microscopic nuclear parameters, b) experimental techniques and facilities employed in measurements, c) the analysis, correlation and interpretation of nuclear data, and d) the compilation and evaluation of nuclear data. Contributions to this Series are reviewed to assure technical competence and, unless otherwise stated, the contents can be formally referenced. This Series does not supplant formal journal publication, but it does provide the more extensive information required for technological applications (e.g., tabulated numerical data) in a timely manner.

PUBLICATIONS IN THE ANL/NDM SERIES

A listing of recent issues in this series is given below. Issues and/or titles prior to ANL/NDM-130 can be obtained from the National Technical Information Service, U. S. Department of Commerce, National Technical Information Service, Technology Administration, Springfield, VA 22161, or by contacting the author of this report at the following address:-

Technology Development Division
Argonne National Laboratory
9700 South Cass Avenue
Argonne, IL 60439
USA

In addition, information on the ANL/NDM report Series can be found on the Internet at the following URL: http://www.td.anl.gov/reports/ANLNDMReports.html. This Internet address contains complete textual and tabular information.

A. B. SMITH AND P. T. GUENTHER
Fast-Neutron Interaction with the Fission Product ^{103}Rh
ANL/NDM-130, September 1993

A. B. SMITH AND P. T. GUENTHER
Fast-Neutron Scattering from Vibrational Palladium Nuclei
ANL/NDM-131, October 1993

A. B. SMITH
Neutron Interaction with Doubly-Magic ^{40}Ca
ANL/NDM-132, December 1993

A. B. SMITH
Neutron Scattering at Z = 50:- Tin
ANL/NDM-133, September 1994

A. B. SMITH, S. CHIBA AND J. W. MEADOWS
An Evaluated Neutronic File for Elemental Zirconium
ANL/NDM-134, September 1994

A. B. SMITH
Neutron Scattering from Uranium and Thorium
ANL/NDM-135, February 1995

A. B. SMITH
Neutron Scattering and Models:- Iron
ANL/NDM-136, August 1995

A. B. SMITH
Neutron Scattering and Models:- Silver
ANL/NDM-137, July 1996

A. B. SMITH
Neutron Scattering and Models:- Chromium
ANL/NDM-138, June 1996

W. P. POENITZ AND S. E. AUMEIER
The Simultaneous Evaluation of the Standards and Other Cross Sections of Importance for Technology
ANL/NDM-139, September 1997

J. T.Daly and D. L. Smith

A Compilation of Information on the $^{31}P(p,\gamma)^{32}S$ Reaction and Properties of Excited Levels in ^{32}S

ANL/NDM-140, November 1997

A. B. SMITH

Neutron Scattering and Models:- Titanium

ANL/NDM-141, July 1997

A. B. SMITH

Neutron Scattering and Models:- Molybdenum

ANL/NDM-142, July 1999

R. E. MILLER AND D. L. SMITH

A Compilation of Information on the $^{31}P(p,\gamma)^{33}Cl$ Reaction and Properties of Excited Levels in ^{33}Cl

ANL/NDM-143, July 1997

R. E. MILLER AND D. L. SMITH

A Compilation of Information on the $^{31}P(p,\gamma)^{28}Si$ Reaction and Properties of Excited Levels in ^{28}Si

ANL/NDM-144, November 1977.

R. D. LAWSON AND A. B. SMITH

Abarex-A Neutron Spherical Optical-Statistical Model Code: A Users Manual

ANL/NDM-145, June 1998.

R. T. KLANN AND W. P. POENITZ

Non-destructive Assay of EBR-II Blanket Elements Using Resonance Transmission Analysis

ANL/NDM-146, August 1998.

A. B. SMITH

ELEMENTAL ABAREX -- A User's Manual

ANL/NDM-147, June 1999.

D. G. NABEREJNEV AND D. L. SMITH

A Method to Construct Covariance Files in ENDF/B Format for Criticality Safety Applications

ANL/NDM-148, June 1999.

A. B. Smith

Neutrons and Antimony:- Physical Measurements and Interpretations

ANL/NDM-149, July 2000

A. B. Smith

Neutrons and Antimony:- Neutronic Evaluations of ^{121}Sb and ^{123}Sb

ANL/NDM-150, July 2000.

A. B. Smith

Fast-neutrons Incident on Holmium

ANL/NDM-151, December 2000.

R. D. Lawson and A. B. Smith

Technical note:- Dispersion Contributions to Neutron Reactions

ANL/NDM-152, April 2001

ANL/NDM-153

FAST NEUTRONS INCIDENT ON HAFNIUM*

by

A. B. Smith
Argonne National Laboratory
Argonne, Illinois

June, 2001

Keywords:
Measured neutron $d\sigma/d\Omega_{el}$ and σ_t for elemental Hafnium, 0.3 → 1.5 MeV and 4.5 → 10.0 MeV. Optical and coupled-channels model interpretations.

---

*This work supported by the United States Department of Energy under contract W-31-109-Eng-38.

TABLE OF CONTENTS

ANL/NDM-153

FAST NEUTRONS INCIDENT ON HAFNIUM

by

Alan B. Smith

Abstract

Total neutron cross sections of elemental Hf were measured from ≈ 0.75 → 4.5 MeV, in steps of ≈ 40 keV and with few-keV resolutions. Differential elastic-scattering cross sections of elemental Hf were measured from ≈ 4.5 → 10.0 MeV, in ≈ 0.5 MeV steps and at 40 scattering angles distributed between ≈ 17^{o} and 160^{o}. Some additional elastic- and inelastic-scattering results were obtained at incident energies of less than 1.5 MeV. These new data were combined with that found in the literature to obtain as comprehensive an experimental data base as possible. It was interpreted in terms spherical-optical-statistical, coupled-channels and dispersive-couple-channels models. The physical characteristics of the resulting potentials are discussed. These potentials are a vehicle for extrapolation, evaluation, interpolation and physical calculation for both basic and applied purposes. Comparisons are made with ENDF/B-6 (MAT 7200).

1. Introductory remarks

Elemental hafnium consists of a complex mixture of odd and even isotopes {^{174}Hf (0.162%), ^{176}Hf (5.206%), ^{177}Hf (18.606%), ^{178}Hf (27.297%), ^{179}Hf (13.629%) and ^{180}Hf (35.100%)} [NDS]. All are highly deformed collective rotors with β_2 values of ≈ 0.2 → 0.3 [Ram+87]. The low-lying structure of the even isotopes is typical of a 0^+, 2^+, 4^+ and 6^+ ($K = 0^+$) ground-state rotational band. The respective excitation energies are very similar; ≈ 0.0, 0.090, 0.3 and 0.6 MeV, respectively. The rotational bands of the two odd isotopes are quite different being based upon $K = 7/2^-$ (^{177}Hf) and $K = 9/2^+$ (^{179}Hf) ground-state rotational bands; although the first excited states, $(9/2^-)$ and $(11/2^+)$ respectively, are at ≈ 0.1 Mev, i.e. at approximately the same energies as those of the even isotopes. This mixture of odd and even isotopes and the complexity of the excited structure makes the measurement and interpretation of the fast-neutron interaction with elemental hafnium difficult. It is probably for that reason that essentially all the experimental knowledge of neutron scattering from elemental hafnium is confined to the present work and a very early and much lower energy Argonne study [SSW70]. The situation is somewhat better

for total cross sections, but even there nothing is known above ≈ 20 MeV. There is very little experimental knowledge of the fast-neutron interaction with the various isotopes. This lack of information is, unfortunately, prevalent throughout this deformed mass region where one would like to understand the details of the neutron interaction with the collective configurations of both even and odd targets.

The hafnium isotopes are well above the conventional fission-yield curves therefore will not be a common applied problem in the context of fission-energy production. However, hafnium does occur with zirconium which is a common reactor structural material, thus the nuclear properties of the hafnium isotopes are of applied interest.

2. Experimental procedures and results

The total-cross-section measurements were made using the conventional mono-energetic-source technique ([SSW70],[NG60]). The method has been widely described, particularly in the above references, and thus it will not be further discussed here. The neutron source was the primary neutron group from the $^{7}Li(p,n)^{7}Be$ reaction. The transmission sample was metallic elemental Hf of greater than 98% chemical purity. Attention was given to in-scattering corrections (negligible) and dead-time effects. The total-cross-section measurements were made from ≈ 0.75 → 4.5 MeV in energy increments of ≈ 40 keV. The incident-neutron resolution was a few keV, and the total uncertainties of the individual values was less then several percent. These total cross-sections are shown in Fig. 2-1. They nicely join the lower-energy values previous obtained at this laboratory [SSW70], as illustrated in Fig. 2-2.

The primary scattering measurements were made using the fast time-of-flight technique with the Argonne multi-detection system long used at this laboratory and extensively described in refs. [CL55], [Smi+92], and refs. cited therein. The scattering sample was a 2 cm long and 2 cm diameter cylinder of high-purity elemental Hf metal placed ≈ 12 cm from a pulsed $D(d,n)^{3}He$ neutron source at a 0^{o} reaction angle. The incident-neutron energy spread at the sample varied from ≈ 300 keV at 4.5 MeV to ≈ 100 keV at 10 MeV. The scattered-neutron resolution was ≈ 450 keV, and thus all of the "elastic" scattering results of the present primary work contained inelastic-scattering contaminations from levels up to excitations of ≈ 450 keV in the various isotopes of the element. This distortion is addressed in the model interpretations, as discussed below. All the scattering measurements were made relative to the standard H(n,p) cross section [CSL83], and corrected for angular resolution, multiple-events and beam attenuation using Monte-Carlo methods [Smi91].

The primary differential "elastic"-scattering measurements were made at ≈ 0.5 MeV intervals from 4.5 → 10.0 MeV. At each energy the measurements were made at 40 angles distributed between ≈ 17^{o} and 160^{o}. The systematic uncertainties were estimated to be ≈ 2 → 3%, and the statistical uncertainties were 2% or less in regions of large cross section, increasing to 10% or more in the extreme minima of the distributions. These "elastic"-scattering results are illustrated in Fig. 2-3, together with their uncertainties. Comments on comparisons with sparse other measured results are given below.

In addition to the above, a number of differential elastic-scattering measurements were made at incident energies of ≈ 0.3 → 1.5 MeV in order to confirm and supplement the earlier work of ref. [SSW70]. These measurements employed the same methods described in ref. [SSW70]. They included some inelastic-scattering distributions which will be discussed below. All of these lower-energy results were obtained relative to the differential elastic-scattering cross sections of elemental carbon [Lan+61]. Energy averages of the "elastic"-scattering low-energy results are illustrated in Fig. 3-3-2. Concurrently, some low-energy differential inelastic scattering measurements were made with emphasis on excitation energies of ≈ 0.1 and 0.3 MeV; i.e. primarily due to the yrast 2^{+} and 4^{+} members of the ground-state rotational bands of the even isotopes. These results are given in Section 3-3, below.

3. Model representations

3-1. Data Base

The elemental neutron-total-cross-section data base was taken from the present work and that reported in the literature, as cited in the reference list. (The cited references with the "t" superscript are sources of total-cross-section data, those with the "s" subscript are sources of scattering data. Both subscripts may be applicable.) In some cases the data found in the literature was discrepant with the body of the total-cross-section information and was abandoned. The accepted experimental data base was ordered by energy and then averaged over energy increments to reduce the number of experimental values and smooth fluctuations. The energy-averaging increments were 0.01 MeV below 0.1 MeV, 0.05 MeV from 0.1 → 0.5 MeV, 0.1 MeV from 0.5 → 5.0 MeV, and 0.2 MeV at higher energies. This composite, energy-averaged, total-cross-section data base is shown in Figs. 3-2-1 or 3-3-1. The individual energy-average-experimental total-cross-section uncertainties are estimated to be several percent, and there clearly is some scatter, particularly about 8 → 10 MeV.

The knowledge of elastic neutron scattering is very largely confined to the present work and to the very early and lower-energy Argonne work of ref. [SSW70]. There are only three

additional distributions reported in the literature; the 1 MeV measurement of ref. [WB54] and the ≈ 7 and 8 MeV distributions of refs. [EHW73] and [HW71]. These three distributions are in qualitative agreement with the Argonne work but quantitative comparisons are thwarted by uncertainties in the scattered-neutron resolution functions. There is, in addition, some knowledge of inelastic neutron scattering from the work of ref. [SSW70] and the lower-energy portions of the present work. The cross sections for the inelastic excitation of the observed ≈ 0.1 and 0.3 MeV levels were combined with the similar values from ref. [SSW70] and averaged over ≈ 0.05 MeV incident-neutron energy intervals. The results are illustrated in Fig. 3-3-3.

Throughout the interpretations the experimental uncertainties provided by the various authors were generally accepted. Despite the present work, the above data base is far from complete. In particular, there is no scattering information from ≈ 1.5 → 4.5 MeV, and none above ≈ 10 MeV. The total cross sections reasonably extend to 20 MeV, but there is nothing at higher energies. There is essentially no experimental knowledge of the fast-neutron interaction with any of the hafnium isotopes, and there appears to be no complimentary experimental information dealing with the (p,p) processes.

3-2. Spherical optical model (SOM)

Clearly, in the context of elemental hafnium, consisting of a number of strongly deformed isotopes, a simple SOM is only a qualitative approximation. However, it does have some basic and applied uses, e.g. as a basis for DWBA calculations. A spirit of the present work is to develop such a qualitative SOM from the experimental data base. The subsequent sections will deal with the more physically appropriate and complex coupled-channels models. There are six isotopes of elemental hafnium, four even and two odd. The energies, spins and parities of the first 10 → 12 levels of each of these isotopes was taken from the Nuclear Data Sheets [NDS]. For the even isotopes this means levels to ≈ 1.3 MeV, and for the odd to ≈ 0.5 MeV. The compound-nucleus contributions to the excitations of each of these discrete levels were calculated using the Hauser-Feshbach statistical formalism ([HF52], [Wol51]) as modified for fluctuation and correlation effects by Moldauer [Mol80]. The calculated compound-nucleus contributions of these levels were combined in a manner that was estimated to be consistent with the experimental resolutions at the various energies. As noted above, the experimental resolutions were too often uncertain. Compound-nucleus contributions from higher-energy levels were treated in a statistical manner using the theory and parameters of Gilbert and Cameron [GC65].

Throughout this work (in both SOM, CCM and DCCM considerations) the real potential was assumed to have a Woods-Saxon form. The surface-imaginary potential was taken to have the derivative-Woods-Saxon form. The experimental data base

used in the model development extended to only 20 MeV, and only to 10 MeV for scattering data. These are relatively low energies so volume-absorption was ignored. A real spin-orbit potential of the Thomas form was used with the parameters fixed to those of ref. [WG86] for the SOM and to the values of refs. [Smi00] and [You86] for the CCM and DCCM derivations. These potential forms are defined in a number of places, for example in refs. [Hod94] and [Hod71].

The SOM interpretations concurrently dealt with the six hafnium isotopes using the computer code ELEMENTAL-ABAREX [Smi99]. Treatment in this inclusive elemental manner requires both scalar and vector potentials. It was assumed that the real vector potential was 24 MeV, the imaginary vector potential 12 MeV, and that the spin-orbit vector potential was zero. These are reasonably values [Hod94] and the vector contributions to the overall potential are small {e.g. $V_r(\text{vector}) = 24 \cdot (N-Z)/A$}, thus reasonable alternate choices of vector strengths will have relatively minor effects. However, it should be made very clear that the SOM parameters cited herein are only scalar parameters to which must be added the above vector contributions. These contributions are properly handled by the SOM code ELEMENTAL-ABAREX.

The SOM geometries were derived by chi-square fitting the above differential-elastic scattering data. It was a four-step procedure long used at this laboratory. First, six parameter fits (real and imaginary potential strengths, radii and diffusenesses) were made. From these the real diffuseness (a_v) was fixed. Next, five parameter fits fixed the real radius (r_v). Herein radii are expressed in the reduced form (r_i) where the full radius is $R_i = r_i \cdot A^{1/3}$, and A the target mass. Four parameter fits then fixed the imaginary radius (r_w) and three parameter fits the imaginary diffuseness (a_w). Unfortunately, there was a lot of scatter in these various parameters and there was a tendency for different behavior in different energy ranges. This is not particularly surprising as the data base is not very comprehensive, the resolutions of the measurements are uncertain and the results include elastic and direct-inelastic scattering not consistent with the concept of the SOM. There was not a reasonable suggestion of an energy dependence of any of these geometric parameters, therefore they were taken to be energy independent with simple averages defining the values. Though the present geometric-parameter uncertainties were large, the values appeared consistent with those established for the similar deformed target ^{165}Ho ([Smi00], [You86]), where the experimental definition is better. Therefore, the better-known ^{165}Ho SOM

geometries were accepted for the remainder of the SOM interpretation [Smi00].

With geometries fixed the data base was extended to include not only the above elastic distributions but also selections of the energy-averaged neutron total cross sections (see Fig. 3-2-1) stretching from 0.1 MeV to 15 MeV, and explicitly including values at the energies of the elastic distributions. In doing so the total-cross-section values were given a weighting 20 times that of the individual differential elastic values. Experience has shown that this is a good compromise in the composite fitting of elastic- and total-neutron cross sections. This elastic-scattering and total-cross-section data base was then chi-square fitted assuming that the real and imaginary scalar strengths had a linear energy dependence. Clearly, it was a four-parameter fit. The final SOM parameters are summarized in Table 1. (Here, as in all potential tables of this work, potential parameters are given to sufficient precisions to permit the accurate calculation of the cited results, they do not necessarily imply parameter uncertainties.) Again, it must be remembered that these are scalar parameters to which must be added the vector components cited above. The energy dependence of the real scalar strength is reasonable for a local-equivalent SOM [PB62]. The imaginary-potential strength increases with energy as one would expect from the opening of additional channels. The magnitudes of the J_v and J_w strengths are reasonably consistent with general trends in this deformed mass region [Smi00]. The real-potential r_v and a_v are on the small side of the average but not abnormally so. The imaginary r_w is reasonable but the the imaginary a_w is somewhat large. This potential gives a very good description of the measured total cross sections, as illustrated in Fig. 3-2-1. The discrepancy between calculated and energy-averaged experimental values is generally no more than several percent (i.e. within the experimental uncertainties alone). At very low energies the calculated results tend to be somewhat higher than the measured values. That is not surprising as the measurements are very old and there is no evidence that any consideration was given to self-shielding effects at low energies. Such self-shielding effects will distort the experimental results toward smaller values in the low-energy region. The effect may be significant but is mitigated in the present case by the multi-isotopic nature of the elemental sample. The SOM leads to large S_o strength functions, about three times those deduced from resonance measurements, and S_1 strength functions about twice those deduced from resonance measurements [MDH81]. These are rather large discrepancies and may reflect the inappropriateness of the SOM. The SOM description of the measured differential scattering data is only qualitative at best. This is not surprising as most of the measured scattering distributions contain large contributions from the direct inelastic excitation of the first few low-lying

levels that are simply inconsistent with the SOM assumption of compound-nucleus inelastic-scattering alone. These direct inelastic contributions are dealt with in the CCM discussed below.

3-3. Coupled-channels Model (CCM)

The isotopes of hafnium are clearly highly deformed rotors [NDS]. Their excited structures are generally described by the unified collective model of Mottelson and Nilsson [MN59]. There are six isotopes; ^{174}Hf (0.162%), ^{176}Hf (5.206%), ^{177}Hf (18.606%), ^{178}Hf (27.297%), ^{179}Hf(13.629) and ^{180}Hf (35.100%). For the present interpretations ^{174}Hf can clearly be ignored due to its very low abundance. Thus one is dealing with an element consisting of ≈ 68% very similar even isotopes, each characterized by a typical 0^+, 2^+, 4^+, 6^+ $K = 0^+$ ground-state rotational-band sequence following the familiar expression [Pre62]

$$E_J = \frac{\hbar}{2I}\{J(J+1) + \delta_{K,1/2}a(-1)^{J+1/2}(J+1/2)\} \qquad (3\text{-}3\text{-}1)$$

A more commonly used form of Eq. 3-3-1 is

$$E(J) = E_o + AJ(J+1) + B[J(J+1)]^2 \qquad (3\text{-}3\text{-}2)$$

given, for example, in ref. [NDS]. The first four levels of the ground-state rotational band in each of the even isotopes are at very nearly the same energy. The remaining ≈ 32% of the element consists of the two odd isotopes, ^{177}Hf ($K = 7/2^-$ [514] ground-state rotational band) and ^{179}Hf ($K = 9/2^+$ [624] ground-state rotational band). In addition, all of these Hf isotopes have a number of other collective rotational and vibrational bands at higher excitation energies [NDS]. The calculated total and "elastic"-scattering cross sections of the minority odd isotopes are somewhat different than those of the majority of even isotopes, but the differences are not large. One does not have available an elemental coupled-channels calculational tool such as ELEMENTAL-ABAREX used in the above SOM context. Therefore the present CCM and DCCM interpretations are based upon a mock even-even hafnium target having the elemental mass of hafnium (178.49) and the level structure reported for ^{178}Hf. This is an approximation but it should be reasonably good. A quadrupole deformation of $\beta_2 = 0.287$ was assumed as it is the weighted average of those values from the even hafnium isotopes [Ram+87]. It was assumed that the ground-state (0^+) and first two excited states (2^+ and 4^+) were coupled in the

calculations. An additional 17 discrete levels to excitations of ≈ 1.5 MeV were included in the calculations. The excitation energies, spins and parities were taken from the Nuclear Data Sheets [NDS]. Compound nucleus contributions to each of these excitations were calculated using the Hauser-Feshbach statistical model as for the above SOM. Contributions from higher-lying excitations were calculated using the formalism and parameters of Gilbert and Cameron [GC65], again as for the above SOM case. All the coupled-channels calculations were carried out using the code ECIS96 ([Ray96], [Tam65]).

The geometric parameters were determined by fitting the differential scattering distributions combining levels in a manner estimated to be consistent with relevant experimental resolutions. This grouping of levels was reasonably certain for the results of the present work, fairly clear for the low-energy results of ref. [SSW70] but uncertain for results in the ≈ 1.0 → 1.5 MeV range of ref. [SSW70]. Therefore, the latter block of experimental data was treated with caution. Following the same progressive fitting procedure outlined above in the context of the SOM, the real and imaginary radii and diffusenesses were again reasonably determined. They were remarkably consistent with the CCM values for holmium reported in refs. [Smi00] and [You86]. However, the latter holmium values were better defined therefore they were accepted for the geometries of the remainder of the hafnium coupled-channels fitting. Using them, two-parameter fits were used to determine the real and imaginary CCM strengths and the respective energy dependencies assuming that they were linear in energy dependence. The resulting description of the energy-averaged total cross section was reasonably good. The calculated values were a few percent too large at 15 → 20 MeV and several percent too large in the 1 → 3 MeV region. With the CCM geometries fixed, representative experimental total cross sections extending from ≈ 0.1 → 20.0 were introduced into the considerations. Slight adjustments of the real and imaginary potential strengths and energy dependencies resulted in a very good description of the total cross section from < 0.1 → 20 MeV as illustrated in Fig. 3-3-1. This final set of CCM parameters is given in Table 2. The agreement between calculated and measured total cross sections is within several percent over the entire energy range. The CCM calculated and measured elastic angular distributions are compared in Fig. 3-3-2. Below ≈ 1 MeV and above 4 MeV the agreement is reasonably good. Between ≈ 1 → 1.5 MeV there are uncertainties regarding experimental resolution. The figure shows three curves for each energy in this region, corresponding to elastic, elastic + first inelastic contributions, and elastic + first and second inelastic contributions. For example, at ≈ 1 MeV the measurements appear to be essentially elastic scattering, while at 1.46 MeV they appear to include both first and second inelastic-scattering groups. The S_o strength functions calculated with the CCM of Table 2 are only slightly larger than those deduced from measurements

[MDH81], just beyond the experimental uncertainty. However, the calculated S_1 values are a factor of two to three larger than indicated by measurements.

The CCM potential of Table 2 was also used to calculate the inelastic excitation cross sections for the observed ≈ 0.09 and ≈ 0.3 MeV levels. About ≈ 68% of these two cross sections are due to the 2^+ and 4^+ members of the ground-state rotational bands of the even isotopes. The remaining ≈ 32% of the contributions were assumed to come from the $K = 7/2^-$ (^{177}Hf) and $K = 9/2^+$ (^{179}Hf) ground-state rotational bands of the two odd isotopes. The calculated results are remarkably close to the measured values as illustrated in Fig. 3-3-3. Attempts were not made to calculate the cross sections for some of higher excitations. The underlying contributing structure is not well known, the resolution of the available experimental information is uncertain, and both the present inelastic results and those of ref. [SSW70] used the ^{7}Li(p,n)^{7}Be reaction as a neutron source at lower energies. That reaction emits a second neutron group that distorts measured values at excitations of ≈> 0.45 MeV.

3-4. Dispersive Coupled-Channels Model (DCCM)

It is well known that there is a dispersion relationship linking real and imaginary potentials and reflecting causality ([Sat83], [Lip66], [Pas67], [Fes58]). This relationship can be expressed in the form

$$J(E)_v = J(E)_{HF} + \frac{P}{\pi} \int_{-\infty}^{+\infty} \frac{J_w(E')}{E - E'} dE' \qquad (3\text{-}4\text{-}1)$$

where J_{HF} is the local-equivalent Hartree-Fock potential, J_w is the strength of the imaginary potential (in volume-integrals per nucleon) and "P" denotes the principle value of the integral. This integral can be broken into surface, ΔJ_s, and volume, ΔJ_{vo}, components

$$\Delta J_s = \frac{P}{\pi} \int_{-\infty}^{+\infty} \frac{J_s(E')}{E - E'} dE' \qquad (3\text{-}4\text{-}2)$$

and

$$\Delta J_{vo} = \frac{P}{\pi} \int_{-\infty}^{+\infty} \frac{J_{vo}(E')}{E - E'} dE'. \qquad (3\text{-}4\text{-}3)$$

Then $J_v(E) = J_{eff}(E) + \Delta J_s(E)$ and $J_{eff} = J_{HF}(E) + \Delta J_{vo}(E)$, where $J_s(E)$ and $J_{vo}(E)$ are surface and volume imaginary-potential strengths, respectively. The Hartree-Fock component is

approximately a linear function of the energy in the range of the present considerations, while at energies above those of the present experiments J_{vo} can be expected to rise slowly with energy. As a consequence, the two components making up J_{eff} can not be experimentally distinguished. In the present work, J_{HF} approaches J_{eff} as ΔJ_{vo} is small in the range of the present measurements. Thus, the effect of Eq. 3-4-1 is to add a surface component to the real Saxon-Woods potential, consisting of some fraction of J_s. The magnitude of this contribution was evaluated from the CCM potential using the methods of Lawson et al. [LGS87]. In doing so it was assumed that the imaginary potential was entirely a surface effect up to 25 MeV, and then fell linearly with energy to zero at 60 MeV. Concurrently J_{vo} was assumed to linearly increase with energy from zero at 25 MeV to 60 MeV where it reached the J_s 25 MeV value and then remained constant to higher energies. The imaginary potential was assumed zero at the Fermi Energy (E_F) and to have a quadratic energy dependence to zero energy. In addition, the entire imaginary potential was assumed to be symmetric about the Fermi Energy [JLM77]. The average E_F was taken to be -7.5 as estimated from the mass tables [Tul90]. With these assumptions the calculated fraction of the surface-imaginary potential was essentially a linear function energy over the energy range of the present interpretations, falling from approximately unity at zero energy to ≈ 0.1 at 20 MeV. This surface component was introduced into the CCM fitting procedure and and the entire fitting process of the above CCM repeated. In doing so the the imaginary geometry and the real diffuseness of the above CCM results were assumed. Thus the fitting involved real and imaginary strengths and real radius. The latter may change as a surface component has been added to the real potential. As for the CCM, the fitting was extended to include representative total-cross-section values from ≈ 0.1 to 20 MeV The resulting potential parameters are given in Table 3. They are the result of a single iteration as the quality of the data base probably does not warrant further iteration. This DCCM potential gave a very good description of the observed neutron total cross sections, as illustrated in Fig. 3-4-1. This potential also gave a representation of the differential elastic- and inelastic-scattering measurements essentially equivalent to those of the CCM and as illustrated in Figs. 3-3-2 and 3-3-3. Thus the available experimental data is not sufficient to distinguish between CCM and DCCM models though the latter is more physically meaningful.

4. Physical comments

The SOM parameterizations of elemental Hf and ^{165}Ho [Smi00] have their useful aspects but are not physically very sound as they give no attention to the strong collective nature of either

of the targets. Thus, it is not particularly surprising that the SOM parameterization of Hf and of the nearby collective target ^{165}Ho [Smi00] are not particularly similar. Both SOM parameterizations are largely based upon total cross sections and the energy dependence of the total cross sections of elemental Hf and ^{165}Ho are qualitatively different (compare Fig. 2-1 with Fig. 3-1-1 of ref. [Smi00]). The CCM potential strengths of elemental Hf (Table 2) and of isotopic ^{165}Hf (Table 3-3-1 of ref. [Smi00]) are quite similar, with differences that are reasonably within the uncertainties of the data bases from which they were derived. The same thing is true of DCCM potential-strength comparisons for the two targets. In both cases the CCM and DCCM real-potential strengths fall with energy as expected from the non-locality of the nuclear force [PB62], while the imaginary potentials increase with energy as more channels open. However, in both cases the imaginary-potential strengths are relatively small as one might expect from a closed-shell target, but neither target is near a closed shell.

It is generally believed that, as the energy of the incident particles increases, the absorption term of the potential makes a slow transition from a surface to a volume contribution ([Hod71], [BG69]). The energy of the onset of this transition is not well defined and is a matter of some debate. However, it is commonly concluded that volume absorption is negligible up to at least 10 MeV, and relatively small even at 20 MeV. In other words, it is negligible or very small over the entire energy range of the present interpretations. Thus it was ignored in all the present model considerations. This is probably not valid for extrapolations to much higher energies, but it should be clearly understood that the potentials of this work are relevant only energies of less than 20 MeV. Indeed, extrapolation of the quadratic potential forms to much higher energies will lead to unphysical results.

The present CCM (in the linear approximation) implies and effective mass, m^*, that can be compared with values deduced from the non-locality of the nuclear forces as discussed, for example, in refs. [BLM54], [Bru+56], [PB62], and [Bet56]. These concepts have been further studied by Brown et al. ([BGG63], [BDS79]) using a dynamic theory of vibrations. It is shown in refs. [BDS79], [MN81] and [Bau+82] that well away from the fermi energy the ratio of the effective mass to the nucleon mass, m, is $\frac{m^*}{m} \approx 0.68$, which is reasonably consistent with nuclear matter estimated [GPT68]. The CCM potential of Table 2 implies a $\frac{m^*}{m}$ ratio of 0.728, which is a little larger than the theoretical estimate, which suggests that the linear energy dependence of the real potential give in Table 2 should be a bit larger. At the same time the zero end point of the CCM of Table 2 is ≈ 175 MeV

which is qualitatively consistent with the results of global estimates [Bau+82]. Given the uncertainties and limitations of the available data, the CCM model seems to be in reasonably agreement with theoretical concepts.

It is well known ([Lan62], [GS58]) that proton and neutron potential strengths are related through the expression

$$J_i = J_i^o \ (1 \pm \xi_i \cdot \eta) \qquad (4\text{-}1)$$

where J_i are potential strengths (expressed as volume-integrals per nucleon), η is the asymmetry (N-Z)/A, "i" may be "v" of "w" for real or imaginary potentials and ξ_i is a constant equal to $\approx$ 0.5 for the real potential and $\approx$ 1.5 for the imaginary potential [Smi97]. The "+" applies to protons and the "-" to neutrons. The present CCM potential (in the linear approximation of Table 2) leads to $J_v^o = 505.9 - 2.870 \cdot E$ Mev-fm^3, which agrees with ^{165}Ho value [Smi00] to within several percent. Eq. 4-1 can be very useful in constructing unified neutron and proton potentials. Unfortunately, the author could find no relevant experimental (p,p) scattering information for Hf, neither could information specialists at the NNDC.

The present CCM and DCCM interpretations assume a $\beta_2 = 0.287$. That value is the average of results deduced from coulomb-excitation studies of the even hafnium isotopes [Ram+87]. β_4 is doubtless a factor in the calculations but fragmentary experimental evidence indicates it is small ($\approx$ 0.05 [Per+92]), thus it was ignored. The deformation of the odd isotopes ($\approx$ 32% abundant) was taken to be the same as that of the even isotopes. That is not known but it is a reasonable assumption as the level excitation energies predicted by Eq. 3-3-3 are reasonably valid with a single value of $\beta_2 = 0.28$. In view of these observations, the limitations of the experimental data base, and the complexities of the "mock" calculational nucleus it was felt that adjustment of β_2 from the above values or inclusion of a β_4 term in the calculations was not warranted. Theoretical considerations, such as the core-polarization model [MBA75], can give guidance as to deformations applicable to neutron, proton, and electo-magnetic processes, particularly for nuclei near shell closures. The hafnium isotopes are not near shell closures and very little is known of the proton interaction with them.

5. Some comparisons with ENDF/B-6

A substantive motivation of the present work was the provision of nuclear data for applications. Thus it is of interest to compare the present results with relevant portions of

the ENDF/B-6 file evaluated file system [ENDF]. The ENDF/B-6 elemental hafnium file (MAT-7200) is approximately a quarter of a century old. Thus it did not have the benefit of recent work, particularly that of the present report, nor did computational models approach the present standards. Despite these limitations, qualitative comparisons indicate that the ENDF/B-6 elemental hafnium evaluation is remarkably good, though its scope is somewhat limited. As an example, the ENDF/B-6 evaluation is compared with the energy-averaged total cross sections of the present work in Fig. 5-1. The agreement is good but for a few-percent discrepancy from ≈ 1 → 3 MeV. The same discrepancy is evident in Fig. 5-2. This small discrepancy may well be the result of over-relying on several total-cross-section data sets that are probably distorted by the self-shielding effect. The elastic-scattering cross sections of the present work are qualitatively similar to those of of the ENDF/B-6 evaluation, as illustrated in Figs. 5-3 and -4. The evaluation seems to have used the results from some ^{182}W calculations to obtain the elastic-scattering distributions, yet the evaluated results are qualitatively consistent with those of the present work. There are few applications that would be sensitive to the differences between these scattering distributions. As noted above, inelastic neutron scattering from hafnium is not well known. At the time of the ENDF/B-6 evaluation models were crude and the only measured values were those of ref. [SSW70]. Given these limitations, the evaluation does reasonably well for the excitation of the first few levels. For example, the evaluation is only ≈ 10 → 15% lower than the excitation of the ≈ 0.09 MeV level shown in Fig. 3-3-3. In the light of the present experimental work, the inelastic-scattering portions of the evaluation should perhaps be somewhat adjusted, but not by large amounts. Generally, the hafnium ENDF/B-6 evaluation is remarkably suitable given its age and the information available at the time. Modern models can extend its scope but major substantive improvements will require significant experimental measurements, as cited below.

6. Summary remarks

Essentially all of the experimental knowledge of neutron scattering from hafnium and/or its isotopes comes from the present work, or early low-energy work from this Laboratory. Many of the neutron total cross sections also came from the present work. Despite these measurements, the present analysis is limited by experimentally uncertainty and very large voids in the experimental data. However, it does provide SOM, CCM and DCCM potentials that can be useful for basic and applied calculation.

Other than the present work and the total cross sections of ref. [PW83], there has been no relevant new experimental information about the interaction of fast neutrons with either elemental or isotopic hafnium for approximately a quarter of a

century! There is essentially no experimental knowledge of neutron total cross sections above ≈ 20 MeV. Neutron scattering over the incident neutron energy interval ≈ 1.5 → 4.5 MeV is unknown and there are no experimental measurements of any kind of neutron scattering above 10 MeV. Furthermore, the energy resolution in some of the early measurements is uncertain. In view of this lack of experimental information, it is recommended that the following measurements be made:-

1. Elemental/isotopic total cross sections up to ≈ 100 MeV.

2. Elemental/isotopic scattering cross sections from ≈ 0.3 → 5.0 MeV.
3. A few elemental/isotopic scattering measurements in the 10 → 30 MeV range.

These experimental recommendations are within contemporary technical capability. Attention should also be given to the provision of isotopic samples. These are highly deformed collective nuclei. An appropriate mechanism for calculation, prediction, interpolation and extrapolation is the coupled-channels model. It seems that no coupled-channels calculational program exists that will concurrently handle a number of the isotopes of an element in the context of an experimental interpretation. Such a code should be developed. There is essentially no knowledge of (p,p) scattering from the isotopes of hafnium. Such a measurement program should be undertaken so as to make possible the derivation of complimentary model parameters. The above shortcomings tend to be chronic in this mass region.

The new experimental data reported in this document have been transmitted to the National Nuclear Data Center, Brookhaven National Laboratory.

Acknowledgments

The author is appreciative of the help given by Drs. R. McKnight, D. Smith, P. Young and J. Raynal. Without their guidance and/or assistance this work would have been much the poorer. The provision of numerical information from the National Nuclear Data Center was essential, particularly the efforts of Ms. M. Blannau.

References

[Bau+82] Bauer M., Hernandes-Saldana E. Hodgson P. and Quintanille J. (1982) J. Phys. G8 525.

[BDS79] Brown G., Dehesa J. and Speth J. (1979) Nucl, Phys. A330 389.

[Bet56] Bethe H. (1956) Phys. Rev. 103 1363.

[BG69] Becchetti F. and Greenlees G. (1969) Phys. Rev. 182 1190.

[BGG63] Brown G. Gunn J. and Gould P. (1963) Nucl. Phys. 46 598.

[BLM54] Brueckner K., Levinson C. and Mahmound H. (1954) Phys. Rev. 95 217.

[Bru56] Brueckner K. (1956) Phys. Rev. 103 1121.

[CL55] Cranberg L. and Levin J., Proc. Conf. on Peaceful Uses of Atomic Energy, Geneva (United Nations Press, New York, 1956).

[CSL83] Nuclear Standards File, IAEA Tech. Report 227, eds. Conde H., Smith A. and Lorenz A. (1983); also the ENDF/B-6 Standards File.

$[DBN68]_t$ Divadeenam M., Bilpuch E. and Newson H. (1968) DA/B 28 3834.

$[EHW73]_s$ Etemad M., Holmqvist B. and Wiedling T. (1973) Report AE-482.

[ENDF] Evaluated Nuclear Data File/B, Version 6. Available from the National Nuclear Data Center, Brookhaven National Laboratory.

[Fes58] Feshbach H. (1958) Ann. Rev. of Nucl. Sci. 8 49.

$[FG71]_t$ Foster D. and Glasgow D. (1971) Phys. Rev. C3 576.

[GC65] Gilbert A. and Cameron A. (1965) Can. J. Phys. 43 1446.

[GPT68] Greenlees W., Pyle G. and Tang Y. (1968) Phys. Rev. 171 1115; see also Phys. Rev. C1 1145.

$[GM73]_t$ Green L. and Mitchell J. (1973) Report WAPD-TM-1073.

[GS58] Green A. and Sood P. (1958) Phys. Rev. 111 1147.

$[Hau67]_t$ Haugsnes J. (1967) DA/B 28 3538.

[HF52] Hauser W. and Feshbach H. (1952) Phys. Rev. 87 362.

[Hod71] Hodgson P. E., Nuclear reactions and nuclear structure (Clarendon, Oxford, 1971).

[Hod94] Hodgson P. E., The nucleon optical model (World Scientific, Singapore, 1994).

$[HW71]_s$ Holmqvist B. and Wiedling T., (1971) Report AE-430.

[JLM77] Jeukenne J., Lejeune A. and Mahaux C., (1977) Phys. Rev. C16 80.

[Lan+61] Langsdorf A. et al. (1961) Argonne National Laboratory Report ANL-5567 (rev.); see also Ann. of Phys. (1961) 12 135.

[Lan62] Lane A. (1962) Nucl. Phys. 55 676; also Phys. Rev. Lett. 8 171.

[LGS87] Lawson R., Guenther P. and Smith A. (1987) Phys. Rev. C36 1298.

[Lip66] Lipperheide R. (1966) Nucl. Phys. 89 97.

[MBA75] Madsen V., Brown V. and Anderson J. (1975) Phys. Rev. C12 1205.

[MDH81] Mughabghab S., Divadeenam M. and Holden N., Neutron cross sections (Academic, New York, 1981).

[MN59] Mottelson B. and Nilsson S. (1959) Danske, K: Vidsnsk. Selsk. mat-fysk., Sjir. 1 No.8.

[MN81 Mahaux c. and Ngo H. (1981) Phys. Lett. 100B 285.

[Mol80] Moldauer P. (1980) Nucl. Phys. A344 185.

[NDS] Nuclear Data Sheets; Browne E. and Junde H. (1998) Nucl. Data Sheets 84 337; Browne E. (1993) Nucl. Data Sheets 68 747; Browne E. (1994) Nucl. Data Sheets 72 221; Browne E. (1994) Nucl. Data Sheets 71 81; Browne E. (1994) 71 617.

[NG60] Newson H. and Gibbons J. Fast neutron physics Vol.-1, Eds. Fowler J. and Marion J. (Interscience, New York, 1960).

[ODW54]$_t$ Okazaki A., Darden S. and Walton R., (1954) Phys. Rev. 93 461.

[Pas67] Passatore G. (1967) Nucl. Phys. A95 694.

[PB62] Perey F. and Buck B., (1962) Nucl. Phys. 32 353.

[Per+92] Rerrins R. et al. (1992) Phys. Rev. C45 1017.

[Rre62] Preston M. Physics of the nucleus (Addison-Wesly, Reading, MA, 1962).

[PW83]$_t$ Poenitz W. and Whalen J., (1983) Argonne National Laboratory Report ANL/NDM-80.

[Ram+87] Raman S., Malarkey C., Miller W., Nester C. and Stelson P. (1987) At. Data and Nucl. Data Tables 36 1.

[Ray96] Raynal J. (1996) The coupled-channels code ECIS96, private communication; see also CEA Report, CEA-N-2772 (1994).

[Sat83] Satchler G., Direct nuclear reactions (Clarendon, Oxford, 1983).

[SSW70]$_{st}$ Sherwood G., Smith A. and Whalen J. (1970) Nucl. Sci. Eng. 39 67.

[Smi91] Smith A., Argonne National Laboratory Memorandum, unpublished (1981).

[Smi+92] Smith A. et al., Argonne National Laboratory Report ANL/NDM-127 (1992); Phys. Rev. C45 (1992) 1260; Z. Phys. A306 (1982) 265; Nucl. Instr. Methods 50 (1977) 277; and references cited therein.

[Smi97] Smith A. (1997) Argonne National Laboratory Report ANL/NDM-147, and references cited therein.

[Smi99] Smith A. (1999) Argonne National Laboratory Report ANL/NDM-147.

[Smi00] Smith A. (2000) Argonne National Laboratory Report ANL/NDM-151.

[Smi01]$_{st}$ Smith (2001) This work.

[Tam65] Tamura T. (1965) Rev. Mod. Phys. 37 679.

[TSB68]$_t$ Tabony R., Seth K. and Bilpuch E, (1964) Phys. Lett. 13 70.

[Tul90] Tuli J. (1990) Nuclear Wallet Cards, Available from the National Nuclear Data Center.

[WB54]$_S$ Walt M. and Barschall H. (1954) Phys. Rev. 93 1062.

[WG86] Walter R. and Guse P. (1986) Proc. conf. on nucl. data for basic and applied science, eds. Young P. et al., vol.-2, p.-277 (Gordon and Breach, New York).

[Wol51] Wolfenstein L. (1951) Phys. Rev. 82 690.

[You86] Young P. (1986) Los Alamos National Laboratory Report LA-10689-PR; also private communication.

Table 1. Elemental hafnium SOM parameters; energies (E) in MeV, dimensions in fermis, strengths in volume-integrals-per-nucleon (J_i) (MeV-Fm^3), and potential depths in MeV. The cited potential strengths are scalar strengths. In addition, there are real and imaginary vector strengths fixed at 24 MeV (real) and 12 MeV (imaginary), as defined in the text.

Real potential

Depth V = 54.3018 - 0.2400·E
Strength J_V = 416.2 - 1.840·E
r_V = 1.199
a_V = 0.553

Imaginary potential

Depth W = 5.3405 + 0.2023·E
Strength J_W = 64.95 + 2.460·E
r_W = 1.266
a_W = 0.815

Spin-orbit potential [WG86]

Depth V_{SO} = 6.0
r_{SO} = 1.103
a_{SO} = 0.56

Table 2. Elemental hafnium CCM parameters; energies (E) are in MeV, strengths J_i in volume-integrals-per-nucleon (MeV-fm^3), potential depths in MeV, and dimensions are in fermis.

Real potential

$V = 48.787 - 0.6319 \cdot E + 0.0240 \cdot E^2$

Strength $J_v = 465.1 - 6.024 \cdot E + 0.2288 \cdot E^2$

(Approx. linear behavior $V = 47.949 - 0.2720 \cdot E$)

$r_v = 1.260$

$a_v = 0.630$

Imaginary potential

$W = 2.805 + 0.3481 \cdot E$

Strength $J_w = 19.5 + 2.419 \cdot E$

$r_w = 1.260$

$a_w = 0.480$

Spin-orbit potential ([Smi00], [You86])

$V_{so} = 6.000$

$r_{so} = 1.260$

$a_{so} = 0.630$

Deformation

$\beta_2 = 0.278$

Table 3. DCCM potential parameters. The dimensionally, the SO-potential, the deformation, and the nomenclature are identical to those of Table 2.

Real potential

$V = 47.887 - 1.0485 \cdot E + 0.069132 \cdot E^2$

Strength $J_V = 467.4 - 10.235 \cdot E + 0.6745 \cdot E^2$

(Approx. linear behavior, $V = 46.769 - 0.4358 \cdot E$)

$r_V = 1.2704$

$a_V = 0.6300$

Imaginary potential

$W = 2.9779 + 0.3605 \cdot E$

Strength $J_W = 20.7 + 2.5059 \cdot E$

$r_W = 1.2600$

$a_W = 0.4800$

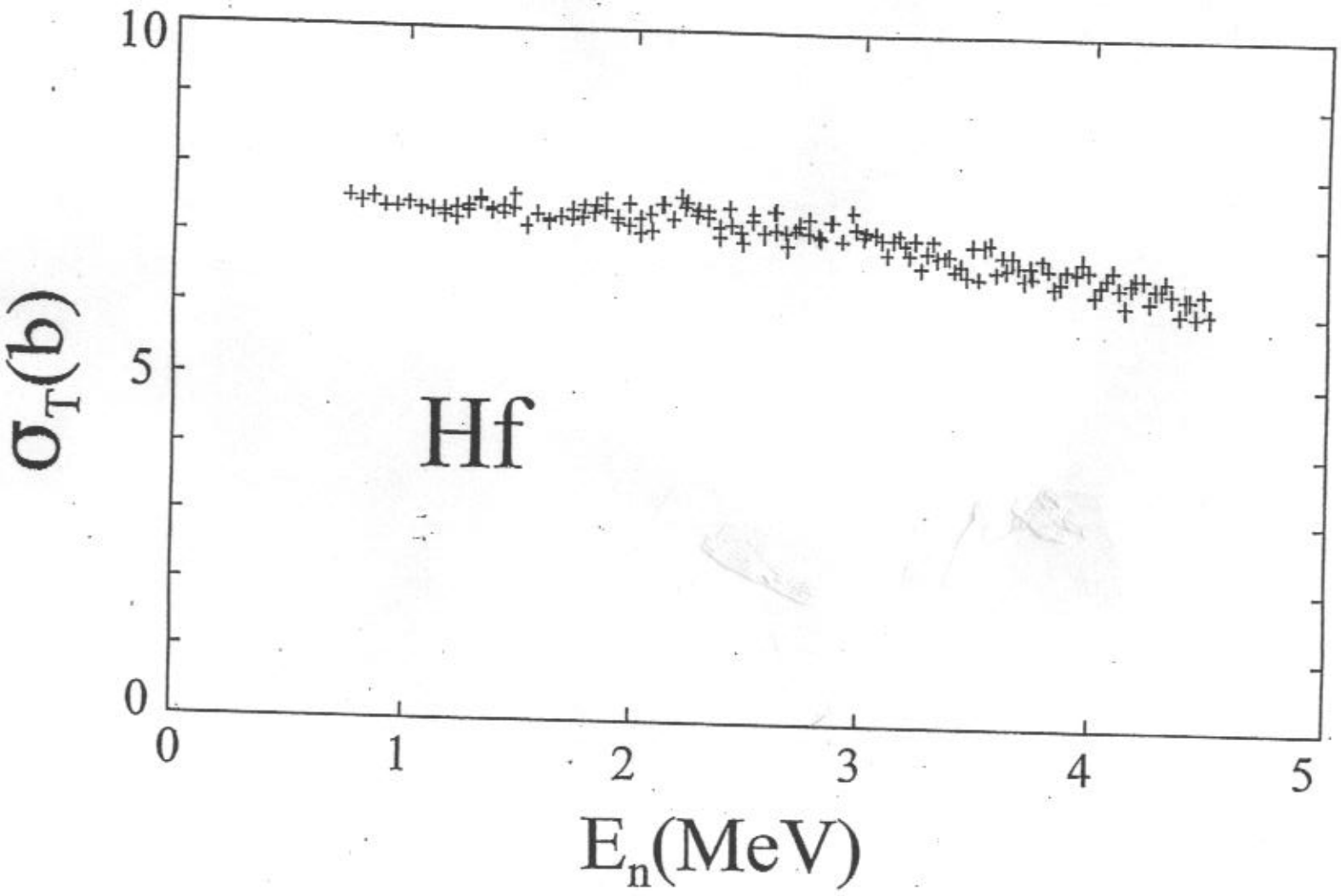

Fig. 2-1. Measured neutron total cross sections of elemental Hf. The present results are indicated by "+" symbols.

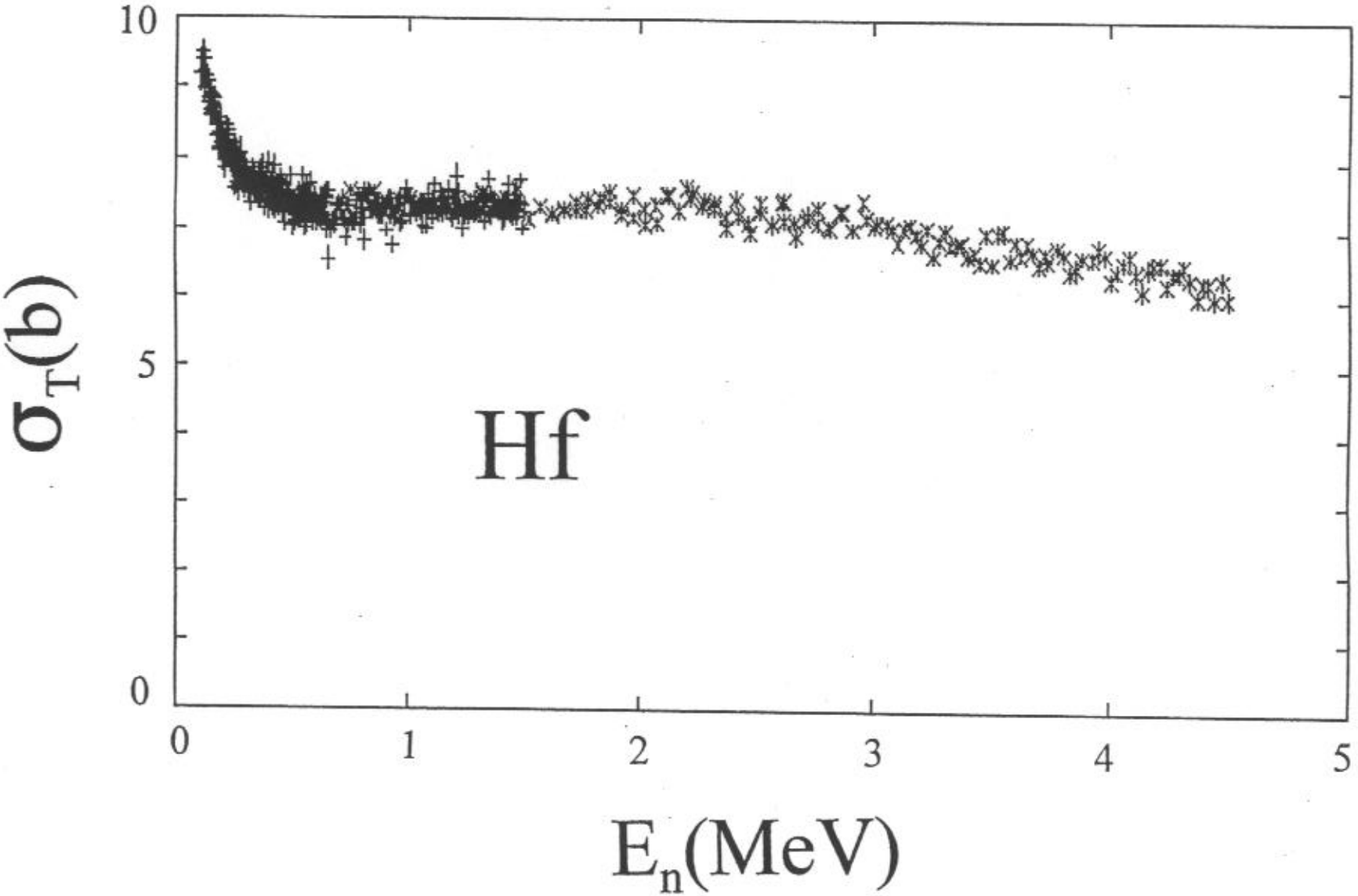

Fig. 2-2. Comparison of measured neutron total cross section of elemental Hf resulting from early work at this institution [SSW70] ("+" symbols) and the present work ("X" symbols).

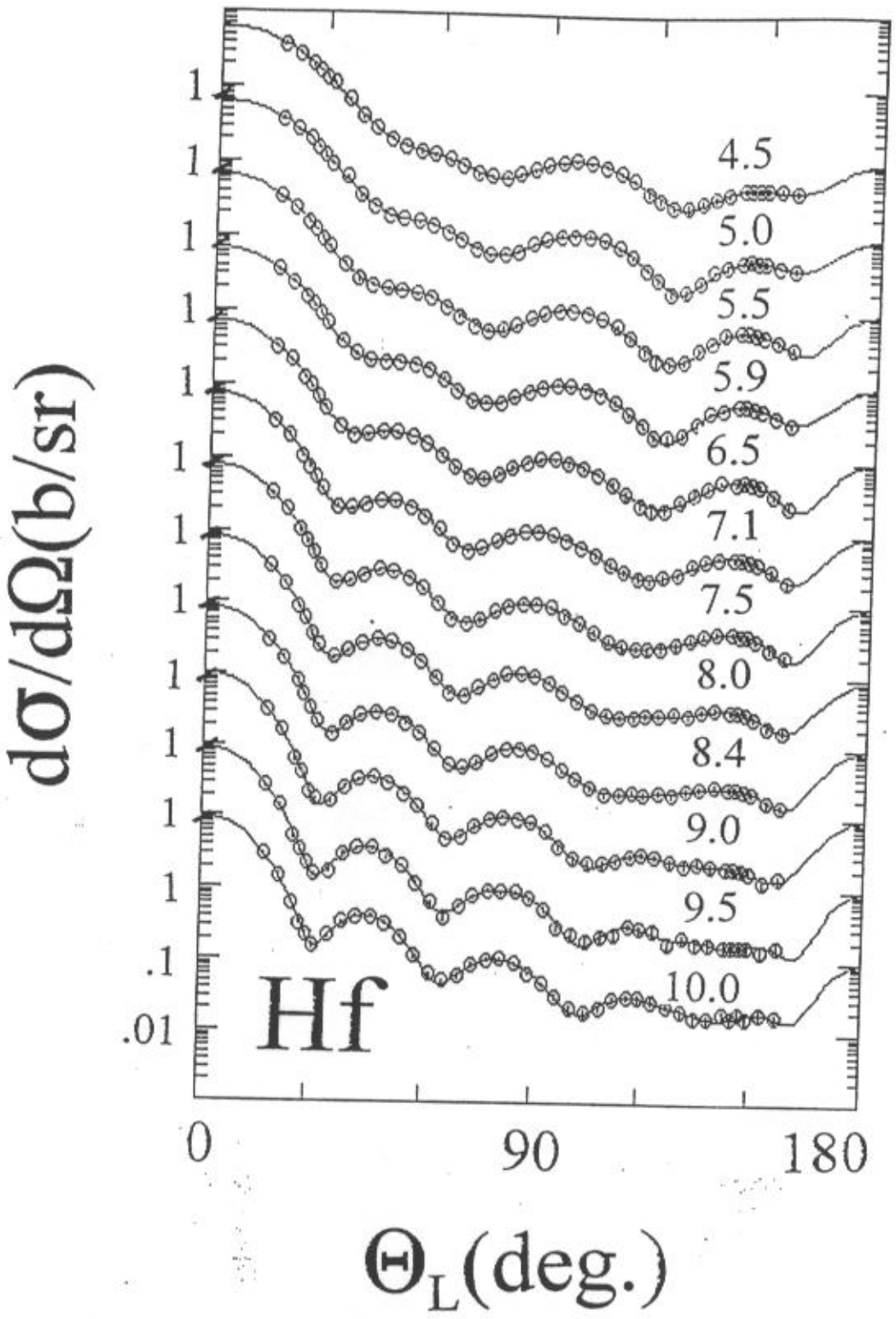

Fig. 2-3. Differential elastic scattering from elemental hafnium. The present experimental results are indicated by symbols and curves denote legendre-polynomial fits to the measured values. Numerical values indicate approximate incident-neutron energies in MeV. Throughout this work, data are shown in the laboratory coordinate system.

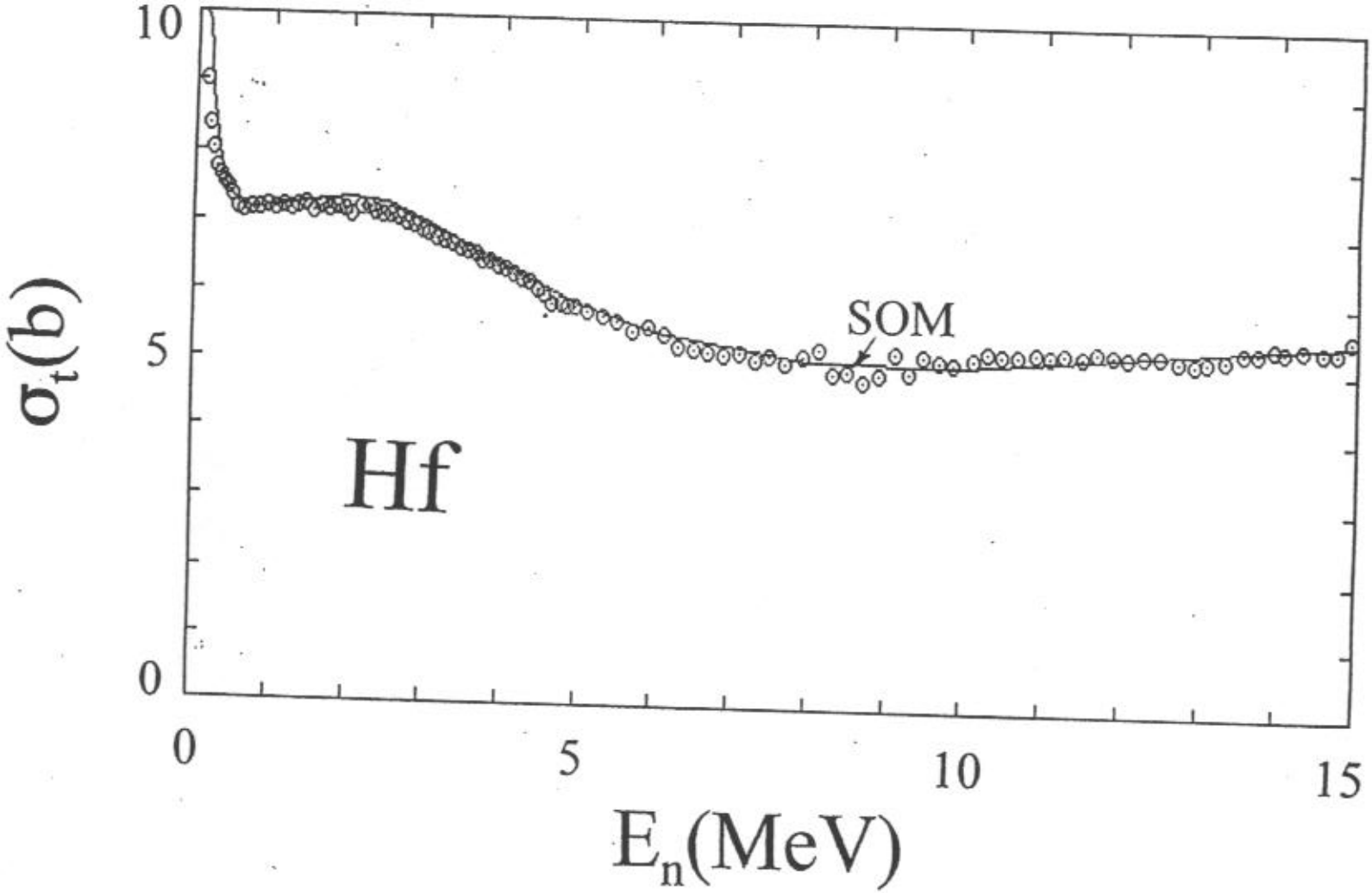

Fig. 3-2-1. Comparison of average-measured (symbols) and calculated (curve) neutron total cross sections of elemental hafnium. The calculations used the SOM of Table 1.

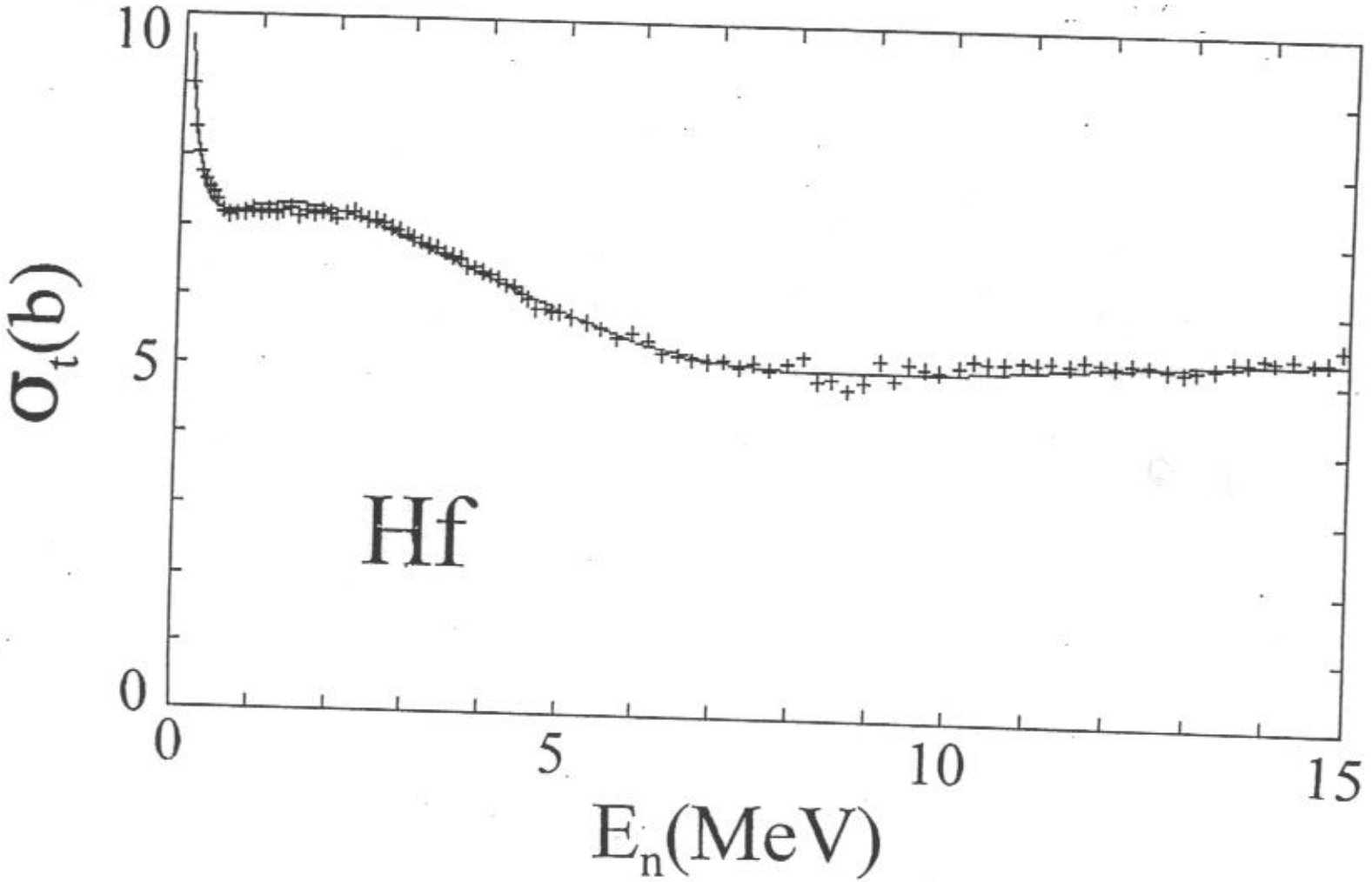

Fig. 3-3-1. Comparison of calculated (curve) and average-measured (data symbols) elemental total cross sections of hafnium. The calculations were made with the CCM potential of Table 2.

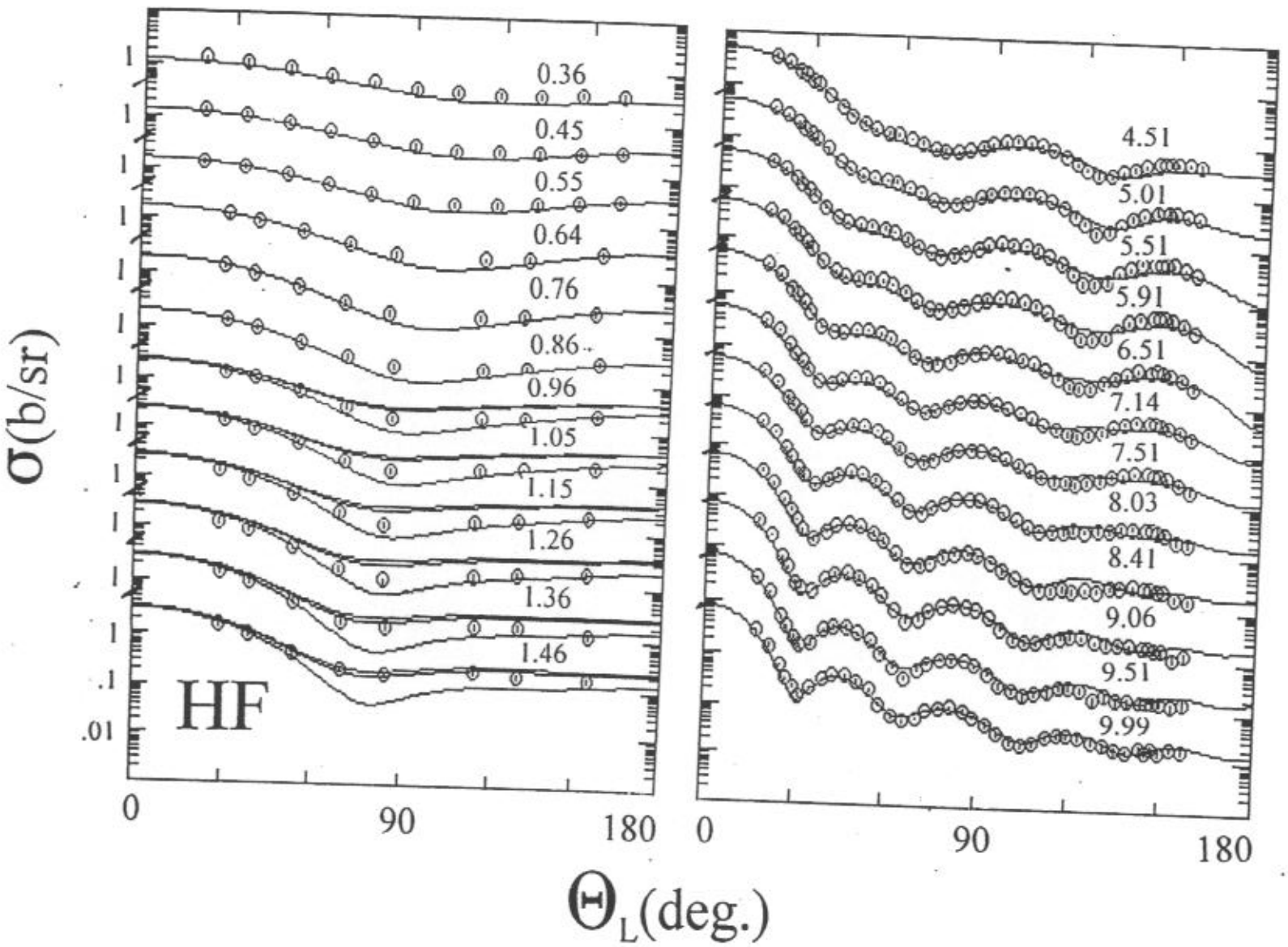

Fig. 3-3-2. Comparison of measured (symbols) and CCM calculated (curves) energy-averaged differential "elastic" scattering cross sections of elemental hafnium. Approximate incident energies are numerically noted in MeV. Where multiple calculational curves are at a given energy they correspond to elastic, elastic + first inelastic, and elastic + first and second inelastic groups as discussed in the text.

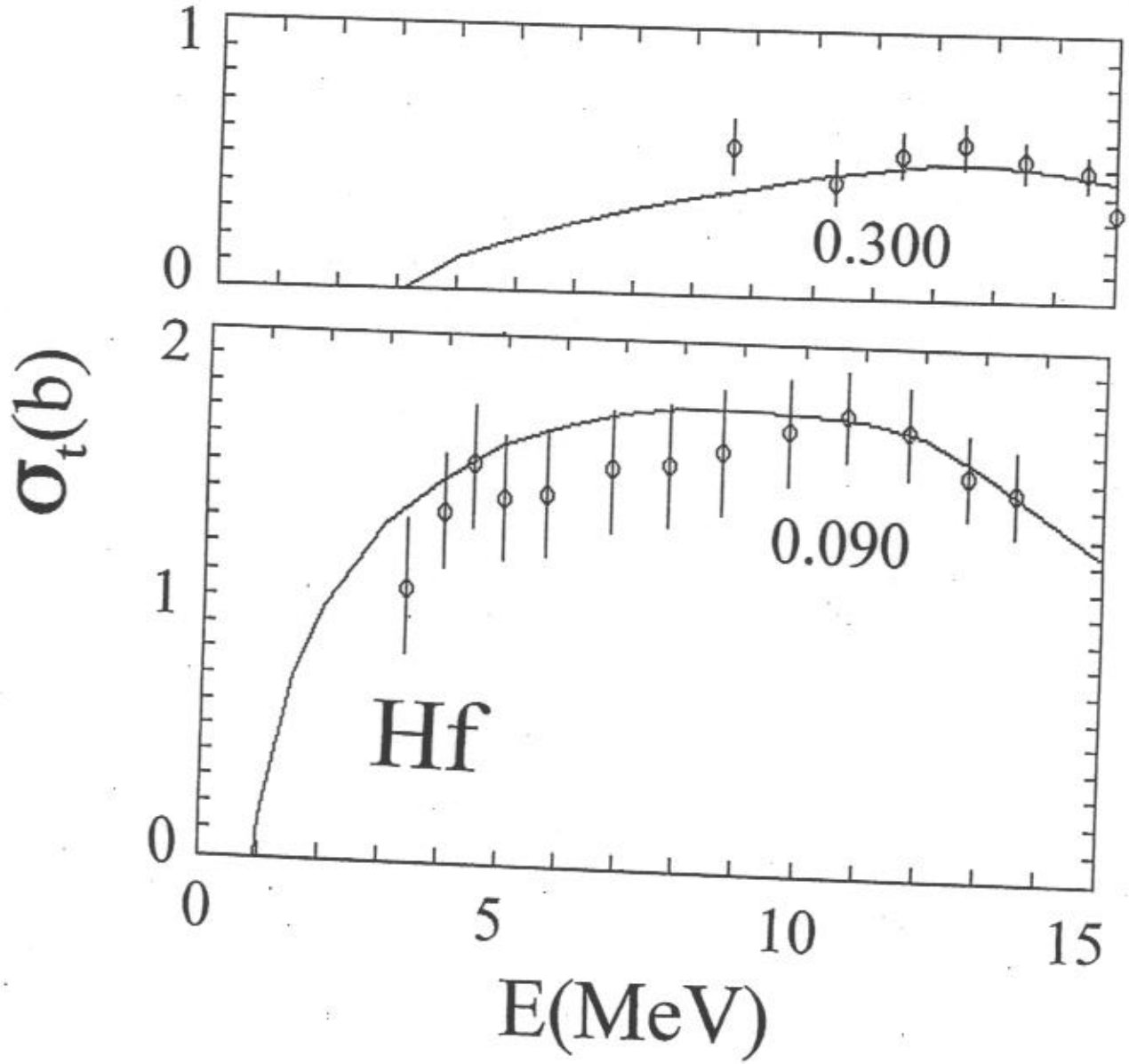

Fig. 3-3-3. Comparison of measured (symbols) and CCM calculated (curves) inelastic-scattering cross sections of the excitations of observed levels at ≈ 0.09 and ≈ 0.30, as described in the text.

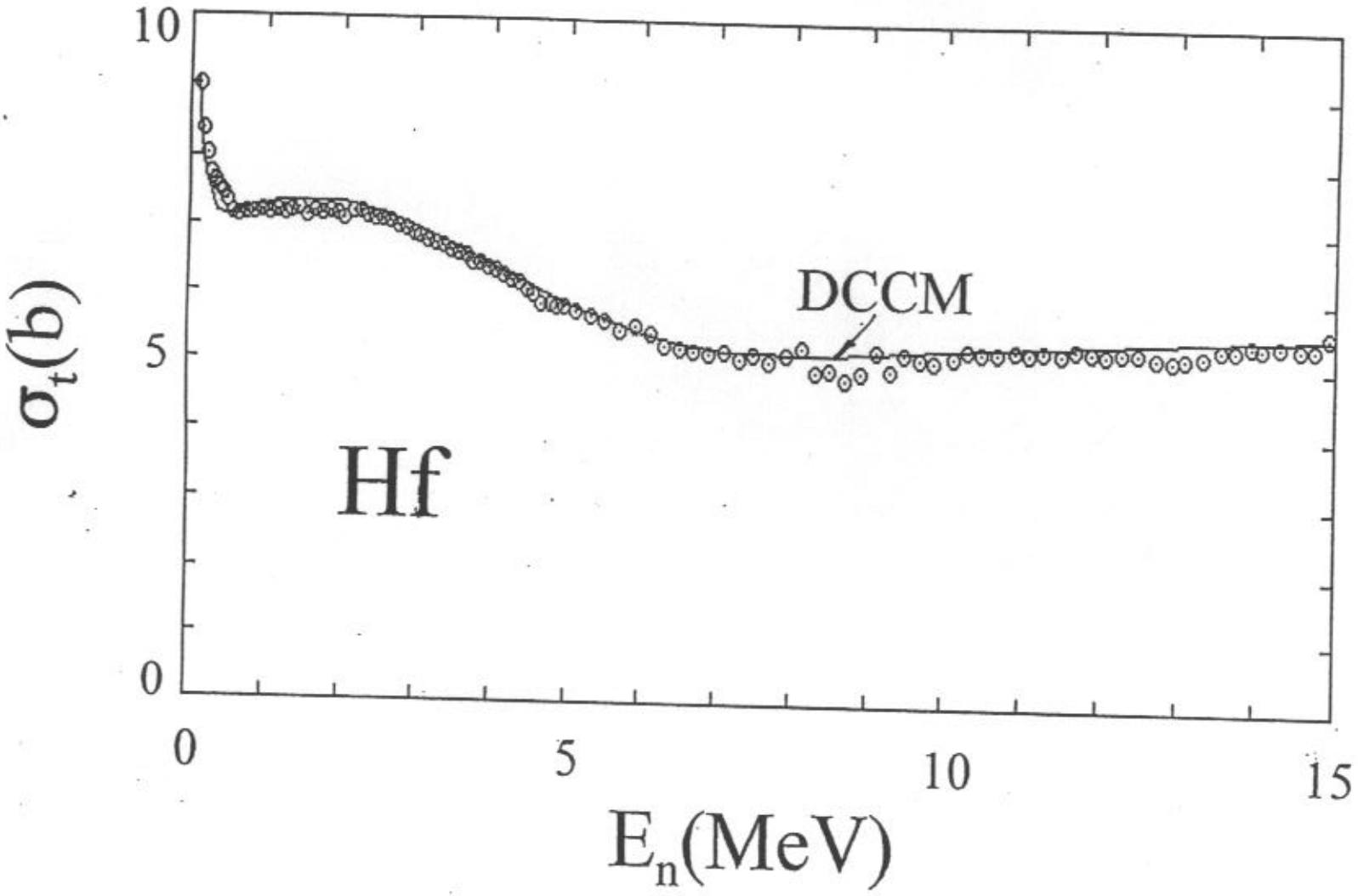

Fig. 3-4-1. Comparison of energy-averaged measured (symbols) and calculated (curve) neutron total cross sections of elemental hafnium. The calculations used the DCCM potential of Table 3.

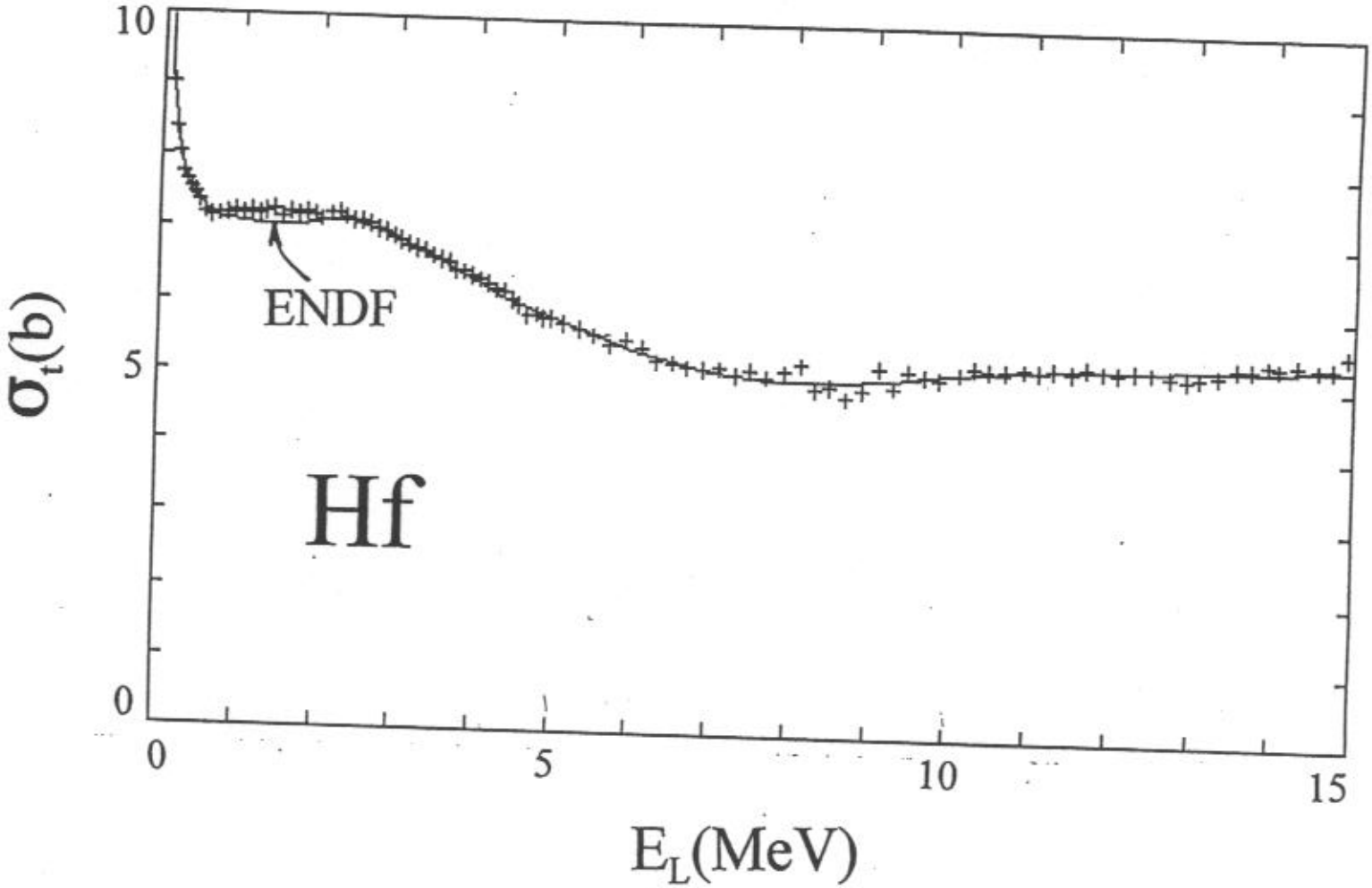

Fig. 5-1. Comparison of ENDF/B-6 total cross sections with measured values. The "+" symbols indicate the energy-averaged experimental data described in the text, and the curve the ENDF/B-6 evaluation.

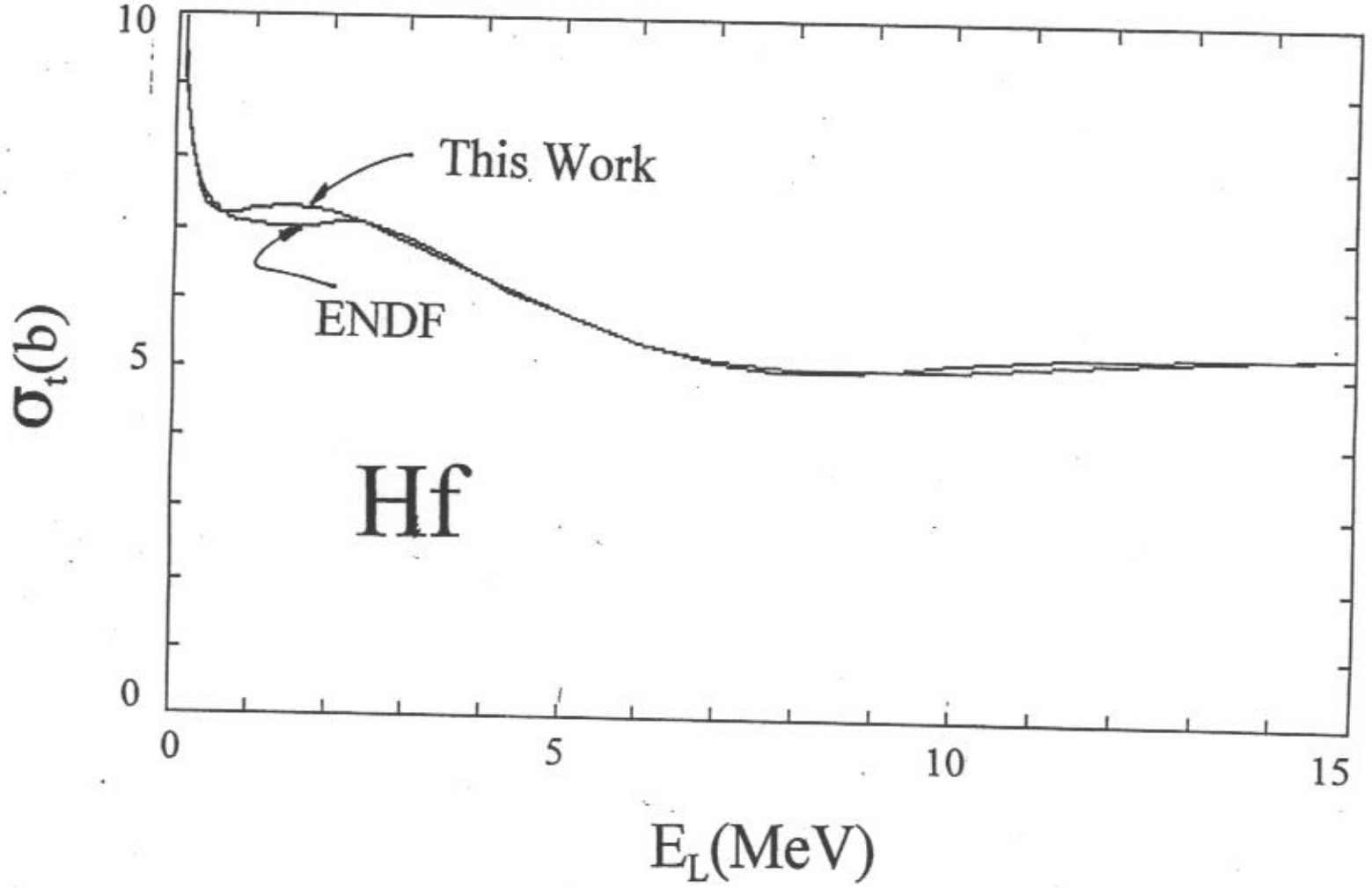

Fig. 5-2. Comparison of the ENDF/B-6 total cross sections evaluation with the results of the above CCM calculations.

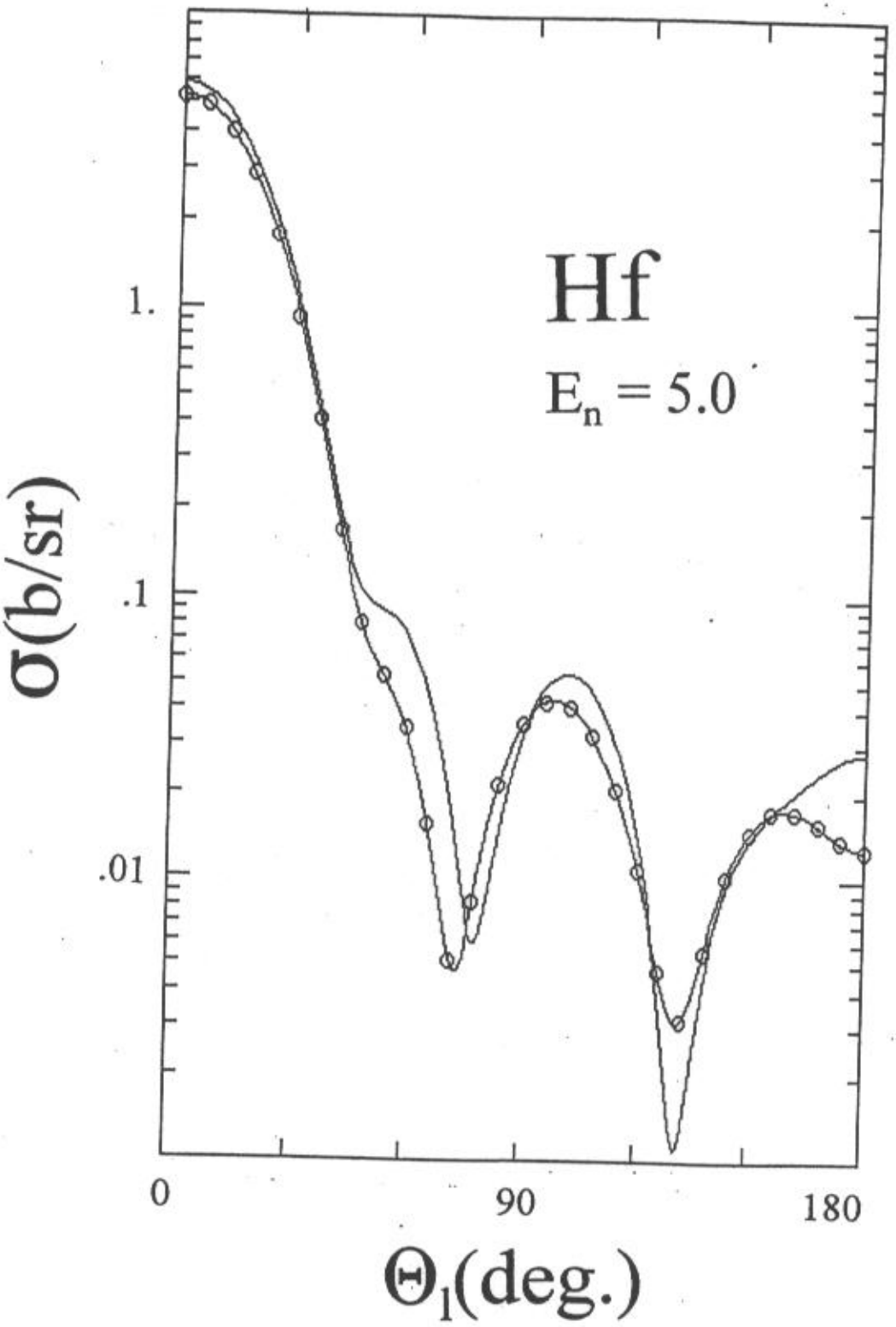

Fig. 5-3. Comparison of ENDF/B-6 elastic scattering at 5 MeV (simple curve) with that calculated with the present CCM (curve with circular symbols).

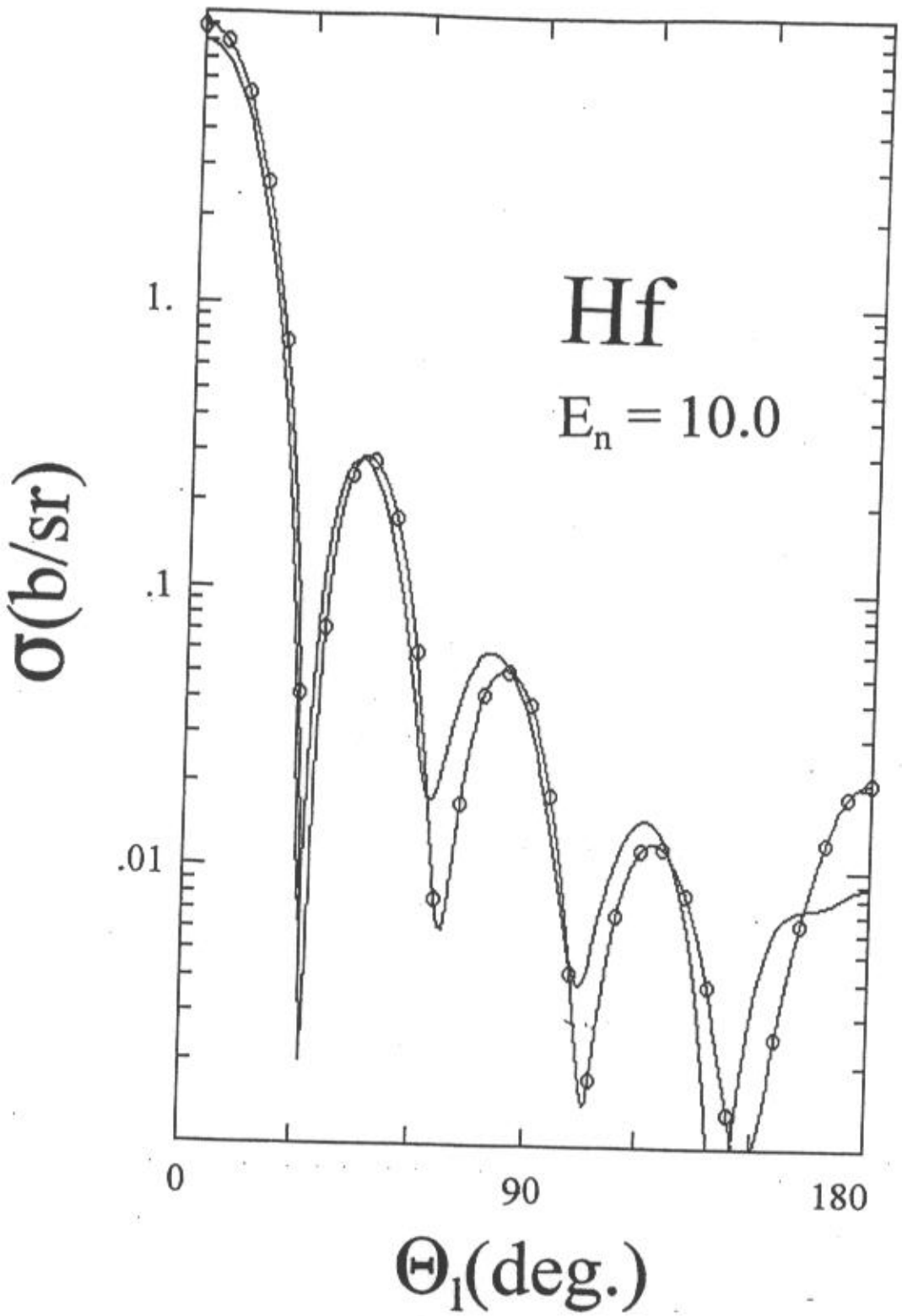

Fig. 5-4. Same comparisons as given in Fig. 5-3, but at 10 MeV.